Chinese Chemical Letters 35 (2024) 108575

Contents lists available at ScienceDirect

Chinese Chemical Letters

journal homepage: www.elsevier.com/locate/cclet

Ratiometric fluorescence probe for accurate detection of Concanavalin A by coupling fluorescent microsphere with boric acid functionalized carbon dots

Mingyue Xie[a], Juan Chen[b], Yufei Wang[a], Bojun Liu[a], Rong-Bin Song[a,c,*], Hong-Min Meng[a,**], Zhaohui Li[a,**]

[a] College of Chemistry, Institute of Analytical Chemistry for Life Science, Henan Joint International Research Laboratory of Green Construction of Functional Molecules and their Bioanalytical Applications, Zhengzhou University, Zhengzhou 450001, China
[b] Zhengzhou Key Laboratory of Forensic Science and Technology, Railway Police College, Zhengzhou 450053, China
[c] School of Ecology and Environment, Zhengzhou University, Zhengzhou 450001, China

ARTICLE INFO

Article history:
Received 19 November 2022
Revised 18 April 2023
Accepted 14 May 2023
Available online 19 May 2023

Keywords:
Concanavalin A
Fluorescent microspheres
Carbon dots
Ratiometric fluorescent assay
Reliability

ABSTRACT

Accurate and sensitive strategies for Concanavalin A (Con A) sensing are conducive to the better cognition of various important biological and physiological processes. Here, by designing dextran-functionalized fluorescent microspheres (DxFMs) and boric acid-modified carbon dots (BCDs) as recognition unit and built-in signal reference respectively, a ratiometric fluorescent detection platform was proposed for Con A detection with high reliability. In this protocol, the BCDs/DxFMs precipitation was formed due to the covalent interactions between *cis*-diol of DxFMs and boronic acid groups of BCDs, thus only fluorescence of BCDs could be detected in the supernatant. When Con A was presented, it could bind to DxFMs through its carbohydrate recognition ability and suppress the subsequent assembly between DxFMs and BCDs, leading to the simultaneous capture of DxFMs and BCDs fluorescence in the supernatant. Since the BCDs content was superfluous, their fluorescence intensities were basically constant in all cases. Based on the unchanged BCDs fluorescence signal and target-dependent DxFMs fluorescence signal in supernatant, the ratiometric detection of Con A was realized. Under optimized conditions, this ratiometric fluorescent platform displayed a linear detection range from 0.125 μg/mL to 12.5 μg/mL with a detection limit of 0.089 μg/mL. Moreover, satisfied analytical outcomes for Con A detection in serum samples were obtained, manifesting huge application potential of this ratiometric fluorescent platform in clinical diagnosis.

Concanavalin A (Con A), a plant lectin extracted from the jackbean, presents a specific affinity toward sugars, such as glucose and their derivatives [1,2]. For this reason, Con A has been implicated in many important physiological and pathological processes like cell communications, leukocytes homing, immune response, malignancy, and metastasis [3–5]. On other level, Con A has also been selected as a protein model for in-depth study of molecular recognition or biological processes that have profound significance for clinical diagnosis and drug development [6,7]. Hence, the sensation of Con A in a sensitive and accurate manner is very pivotal for understanding its diversified functions in these complicated courses.

The reported methods for Con A detection mainly include electrochemiluminescence [8], UV–vis spectroscopy [9], fluorescence spectroscopy [10–12], and surface plasmon resonance [13]. Among them, fluorescence assay occupies a large proportion on account of its simplicity of realization, facile visualization, and real-time analysis features [14]. As a typical fluorescence sensing strategy for Con A, the sugar-labeled fluorescent materials have been used as recognition and signal elements, which can be aggregated to generate fluorescence loss due to the polyvalent interactions between Con A and sugars on the different surfaces of fluorescent materials. Notably, the sensitivity of this sensing strategy is highly associated with the fluorescent properties of the selected signal unit. Compared to the commonly used fluorescent materials like Au nanoparticles [15], semiconductor quantum dots (QDs) [16], Ag nanoclusters [17], Ag nanoparticles [18] and alloy nanoparti-

* Corresponding author at: College of Chemistry, Institute of Analytical Chemistry for Life Science, Henan Joint International Research Laboratory of Green Construction of Functional Molecules and their Bioanalytical Applications, Zhengzhou University, Zhengzhou 450001, China.
** Corresponding authors.
E-mail addresses: rbsong@zzu.edu.cn (R.-B. Song), hmmeng2017@zzu.edu.cn (H.-M. Meng), zhaohui.li@zzu.edu.cn (Z. Li).

https://doi.org/10.1016/j.cclet.2023.108575
1001-8417/

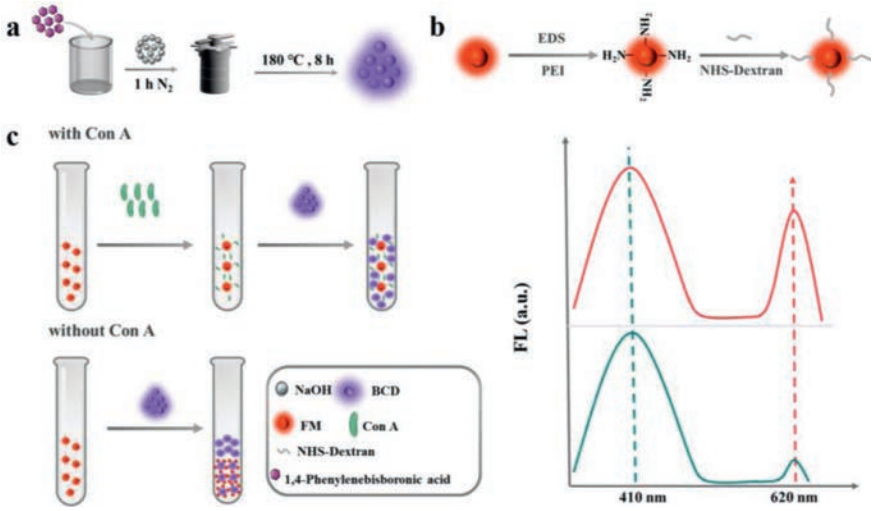

Scheme 1. (a) Schematic depiction of the strategy for fabrication of boronic acid functionalized carbon dots; (b) the preparation process for DxFMs; (c) working principle of the system for Con A assay.

cles [19,20], the fluorescent microspheres (FMs) [21] that converge hundreds of QDs seem to be good alternatives due to the improved fluorescence intensities, optical and colloidal stabilities.

Despite the use of FMs as signal unit, however, the above-mentioned sensing strategy with turn on or turn off variations in the fluorescence intensity is easy to be affected by many factors, including instrument fluctuation, microenvironment perturbation and distribution variation of fluorescent material, leading to the possibility of false-positive error. Thereby, the ratiometric sensing concept that is capable of providing built-in self-calibration for minimizing false-positive error should be taken into consideration [22]. In general, a ratiometric fluorescence sensor usually covers two signals at two or more different wavelengths. To realize this goal, another fluorescent material is required to serve as internal reference except for FMs. Recently, carbon dots (CDs) [23–26] have flourished in the field of fluorescence biosensor due to the splendid luminescence property, good biocompatibility, and easy availability. The abundant CDs species can allow tremendous flexibility to choose one that has the same excitation wavelength with FMs but distinct fluorescence emission peak for simplifying the analysis process. More importantly, CDs possess abundant surface functional groups, which offer the likelihood to interact with sugar-labeled FMs and build relationship with the Con A.

Herein, we have developed a ratiometric fluorescence platform with one excitation wavelength for sensitivity and reliability analysis of Con A *via* the coupling of boric acid-modified CDs (BCDs) and dextran-functionalized FMs (DxFMs). As shown in Scheme 1, the BCDs could bind with DxFMs *via* the covalent interaction between boronic acid groups and *cis*-diol in dextran to form precipitation. In the presence of Con A, it could preferentially bind to dextran and relieve the formation of BCDs/DxFMs precipitation due to its carbohydrate recognition ability, achieving two fluorescence emissions from the DxFMs (620 nm) and BCDs (410 nm) in the suspension. In contrast, all of DxFMs have been combined with BCDs, leading to the lacking of DxFMs in the suspension and the disappearance of fluorescence emission at 620 nm. On the premise of excessive BCDs, we have realized the ratiometric fluorescence detection of Con A with satisfied performance by the relationships between constant BCDs emission and target-dependent DxFMs emission. With advantages of high brightness, rapid response and ratiometric fluorescence, this ratiometric fluorescence platform is expected to become a simple and effective tool for the capture of quantitative information in complicated biological and physiological processes.

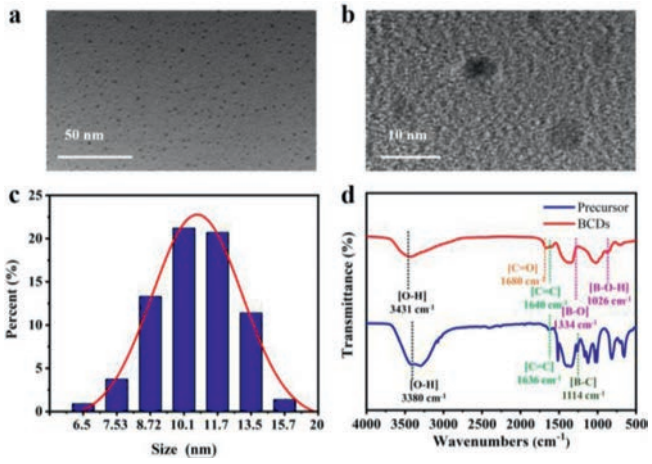

Fig. 1. Characterization of BCDs. (a) The TEM images of BCDs, scale bar: 50 nm; (b) The TEM images of BCDs, scale bar: 10 nm. (c) The size distribution of BCDs. (d) The FT-IR spectra of BCDs and precursor.

The BCDs were prepared by a modified hydrothermal method according to a previous work [27]. The morphologies and sizes of the prepared BCDs were investigated by TEM and DLS. The results showed that the prepared BCDs were spherical and well dispersed, and the TEM diameter of BCDs is about 4.2 nm (Figs. 1a and b). As can be seen in Fig. 1c, the hydrodynamic diameter distribution of BCDs ranged from 6.0 nm to 15.6 nm with an average diameter of 9.8 nm. To study the surface functional groups and compositions of the BCDs, its FTIR spectrum was investigated. As shown in Fig. 1d, the FT-IR spectrum (red curve) of BCDs exhibits distinct absorption bands at 3431, 1680, 1640, 1334, and 1026 cm^{-1}, which can be attributed to are assigned to the O–H stretching vibration, C=O stretching vibrations, C=C stretching vibrations, B-O stretching vibration and B-O-H deformation vibration, respectively. While the FT-IR spectrum (blue curve) of the precursor, exhibits distinct absorption bands at 3380, 1636, 1114 cm^{-1}, which can be attributed to the O–H stretching vibration, C = C stretching vibrations and C-B stretching vibration, respectively. The results demonstrated that there were abundant of boronic acid groups on the surface of BCDs, which was beneficial for Con A detection.

The prepared DxFMs were also characterized by SEM and DLS assay. Compared to FMs in Fig. S1a (Supporting information), there

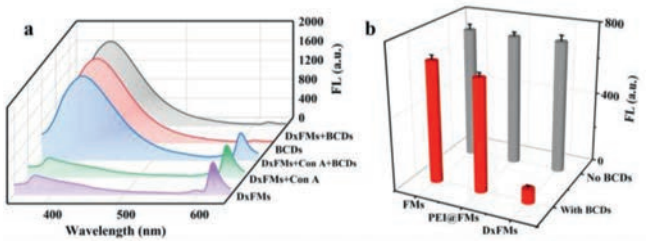

Fig. 2. (a) The fluorescence emission spectra of BCDs, DxFMs and DxFMs in the presence of Con A or BCDs ($\lambda_{ex} = 330$ nm). (b) The fluorescence emission intensity of FMs, PEI@FMs, DxFMs before and after reaction with BCDs.

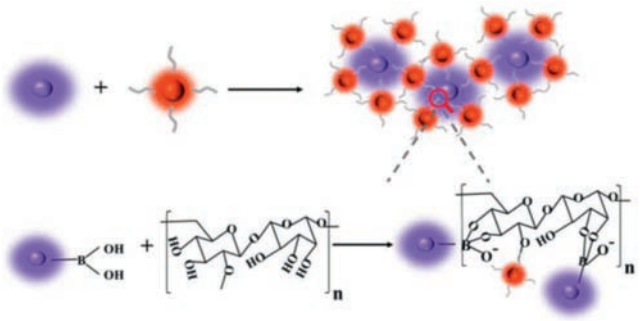

Scheme 2. Schematic diagram illustrating of the covalent binding between *cis*-diols of dextran and boronic acid on the surface of BCDs lead to the assembly of BCDs and DxFMs.

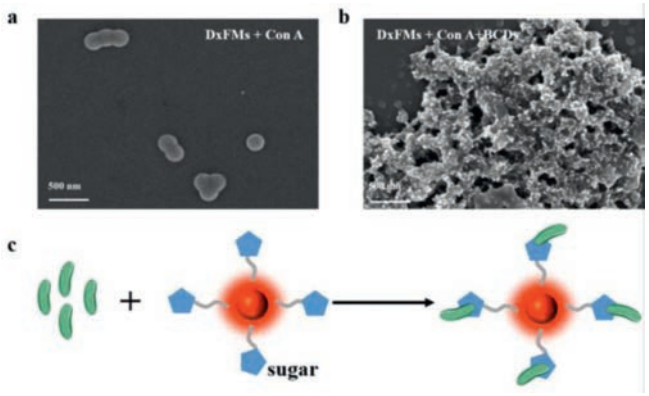

Fig. 3. The SEM image of DxFMs after reaction with Con A (a) and with BCDs (b), scale bar: 500 nm. (c) The schematic diagram illustrating of DxFM reacting with Con A.

were obvious inclusions on the surface of PEI@FMs (Fig. S1b in Supporting information). And compared with PEI@FMs, the surface of DxFMs was further coated by dextran (Fig. S1c in Supporting information). Moreover, the average hydrodynamic diameters were almost in agreement with the SEM results (Figs. S1d-f in Supporting information). The prepared DxFMs were further investigated by measuring the zeta potential. As shown in Figs. S1h-j (Supporting information), the zeta potential of FMs, PEI@FMs and DxFMs was -29.5 ± 1.6 mV, 51.6 ± 2.8 mV and -3.97 ± 1.5 mV, respectively, indicating that DxFMs was successfully prepared. What is more, in order to validate the claims, the energy-dispersive X-ray spectroscopy of BCDs (Fig. S2a in Supporting information) and DxFMs (Fig. S2b in Supporting information) have been provided.

Optical properties of BCDs and DxFMs were measured. As shown in Fig. S3a (Supporting information), an emission peak could be observed at 410 nm for BCDs under 330 nm excitation. DxFMs showed an obvious emission peak at 620 nm with the excitation wavelength of 330 nm (Fig. S3b in Supporting information). These results demonstrated that BCDs and DxFMs could be excited by same wavelength, which was suitable for the building of ratiometric fluorescent sensing platform. In addition, the UV–vis absorption of BCDs (Fig. S3c in Supporting information) and their precursors as well as the fluorescence intensity of DxFMs were presented in Fig. S3d (Supporting information).

To investigate the feasibility of BCDs and DxFMs based probe for Con A assay, the fluorescence intensity at 410 nm and 620 nm under different conditions were recorded. In our design, BCDs was far excessive and its fluorescence intensity could be basically unaffected by Con A, therefore it could be used as the internal reference. As shown in Fig. 2a, we could observe an obvious fluorescence emission peak at 620 nm for DxFMs, and its intensity was almost unchanged after the addition of Con A into DxFMs solution. Moreover, the fluorescence intensity was also slightly decreased with the further addition of BCDs into the DxFMs + Con A solution. However, if the BCDs were directly added into DxFMs solution, we found that the fluorescence intensity at 620 nm decreased significantly. As regards to BCDs, the intensities of its fluorescence emission peak at 410 nm kept constant during all tests, suggesting that its content was enough to serve as internal reference. Fig. 2b illustrated that BCDs could specifically bind to DxFMs but not FMs or PEI@FMs. These results indicated that our system could be used for ratiometric detection of Con A.

The related sensing mechanism was inferred as described in Scheme 2. Both boric acid and Con A can bind dextran on the surface of DxFMs *via* the covalent interaction between boric acid and *cis*-diol as well as the affinity of Con A towards carbohydrate ligands, respectively [28,29]. The abundant boric acid groups would induce the crosslink between DxFMs and BCDs, leading to the formation of DxFMs/BCDs precipitation. However, one Con A tetramer only has four sugar binding sites, the crosslink density between DxFMs and Con A is very low and the formed DxFMs/ConA aggregations would disperse in the suspension. To verify as-mentioned speculation, we detected the aggregations by SEM assay. As shown in Fig. 3a, only small nanoparticles consisting of 2 or 3 FMs were formed in the presence DxFMs and Con A, while the aggregation with crosslinked network structure was found in the presence of DxFMs and BCDs (Fig. 3b). Fig. 3c showed the schematic diagram illustrating of DxFM reacting with Con A. On these contexts, the existed Con A can bind with DxFMs and retained a part of DxFMs in the suspension, achieving two fluorescence emissions from DxFMs and BCDs. In contrast, all of DxFMs would exist in DxFMs/BCDs precipitation, leading to the lacking of fluorescence emissions of DxFMs for the suspension. On the premise of excessive BCDs, the ratiometric fluorescence detection of Con A was realized.

Under the optimized conditions (Figs. S4-S7 in Supporting information), the performance of the sensor was measured. As shown in Fig. 4a, the fluorescence intensity of BCDs at 410 nm remained stable and the fluorescence intensity of DxFMs at 620 nm increased obviously with the increase of Con A. Fig. 4b exhibited the relationship between the value of F_{620}/F_{410} and the concentration of Con A. There was a good linear relationship between Con A and F_{620}/F_{410} in the range of 0.125–12.5 μg/mL ($R^2 = 0.9991$) with a detection limit of 0.089 μg/mL (Fig. 4c). Compared with other previously reported methods, the detection performance of this ratiometric fluorescent probe showed lower LOD for Con A detection (Table S1 in Supporting information). In addition, photos after the reaction completed were collected. It could be clearly seen that with the increase of Con A concentration (from left to right), the precipitation gradually decreased and the fluorescence of the supernatants gradually increased (Fig. 4d).

To investigate the specificity of the system, we evaluated the effects of potential interfering substances in serum, such as Fe^{3+},

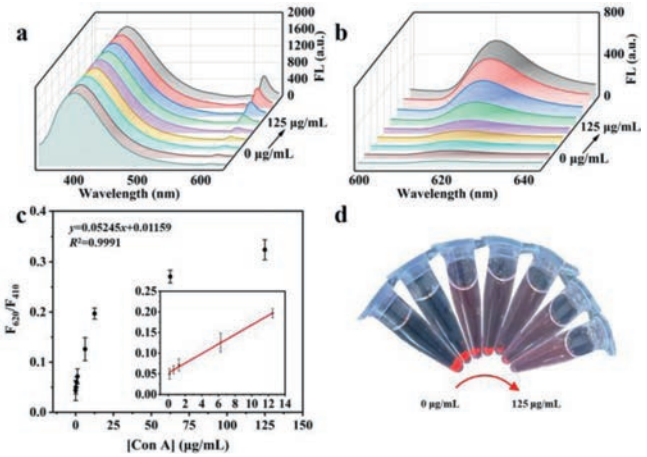

Fig. 4. (a) The fluorescence emission spectra of DxFMs reacting with different concentrations of Con A. (b) The fluorescence emission spectra of DxFMs reacting with different concentrations of Con A at 600–645 nm. (c) The scatter diagram of F_{620}/F_{410} corresponding to (a) and the linear relationship between the concentration of Con A and F_{620}/F_{410}. (d) The photo of DxFMs reacting with different concentrations of Con A under ultraviolet lamp ($\lambda = 365$ nm).

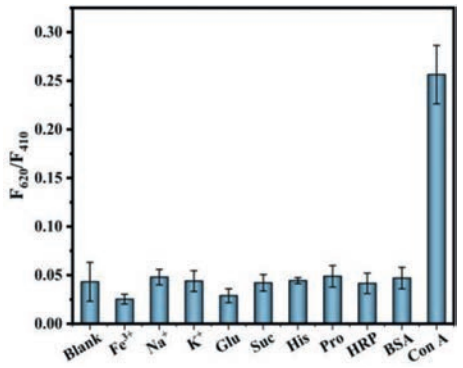

Fig. 5. The selectivity of the ratiometric fluorescent sensing method toward various potential interfering substances.

Table 1
Analytical results of Con A in 10% serum samples.

Sample	Spiked (μg/mL)	Found (μg/mL)	RE (%)	RSD (%) ($n = 3$)
10% Serum	0	0	——	——
	4	4.3	107.5	4.4
	8	8.5	106.3	4.3
	12	12.5	104.2	3.6

Na^+, K^+, histidine (His), L-proline (Pro), horseradish peroxidase (HRP) and bovine serum albumin (BSA), and their concentrations were 1 mmol/L. The fluorescence response of these interfering substances was much lower than that of Con A (Fig. 5). However, *cis*-diols in glucose and sucrose may react with BCDs and interfere the detection, so we chose 1 mmol/L glucose which was slightly higher than that of the 10-fold diluted normal blood sugar concentration to carry out the experiment. The results showed that 1 mmol/L glucose and sucrose did not affect the detection, indicating that the sensing system was not interfered by glucose in the actual sample (10% serum).

To further investigate the practical application potential of this method, Con A in fetal bovine serum was detected using a recovery method. When 4, 8 and 12 μg/mL of Con A were added into 10% fetal bovine serum, the recoveries were 107.5%, 108.8% and 104.2%, and the relative standard deviations ($n = 3$) were 4.4, 4.3 and 3.6, respectively (Table 1). These results demonstrated that the ratiometric fluorescence biosensing method has the potential to quantitatively determine Con A in clinical serum samples.

In summary, we have successfully fabricated a novel and reliable ratiometric fluorescence sensing method for Con A detection. In this protocol, BCDs could bind with DxFMs *via* the covalent interaction, resulting in the formation of precipitation. While, Con A could preferentially bind to DxFMs through carbohydrate recognition ability and suppress the subsequent assembly between DxFMs and BCDs, leading to the simultaneous capture of DxFMs and BCDs fluorescence in the supernatant. Since the BCDs content was superfluous, their fluorescence intensities were basically constant. Based on the unchanged BCDs fluorescence signal and target-dependent DxFMs fluorescence signal, the ratiometric signal was easily obtained for Con A detection. Results showed that this analytical method exhibited a lower detection limit with acceptable simplicity. Notably, the ratiometric system was applied to the determination of Con A in serum with satisfactory results, which suggests a promising possibility towards detecting diverse biological molecules.

Declaration of competing interest

The authors declare that they have no known competing financial interests or personal relationships that could have appeared to influence the work reported in this paper.

Acknowledgments

This work was supported by the Key Project of Science and Technology of Henan Province (No. 212102310334), National Natural Science Foundation of China (Nos. 21974125, 22174131).

Supplementary materials

Supplementary material associated with this article can be found, in the online version, at doi:10.1016/j.cclet.2023.108575.

References

[1] L.N. Cella, W. Chen, N.V. Myung, et al., J. Am. Chem. Soc. 132 (2010) 5024–5026.
[2] A. Samanta, M.C.A. Stuart, B.J. Ravoo, J. Am. Chem. Soc. 134 (2012) 19909–19914.
[3] R.A. Dwek, Chem. Rev. 96 (1996) 683–720.
[4] G.E. Ritchie, B.E. Moffatt, R.B. Sim, et al., Chem. Rev. 102 (2002) 305–320.
[5] N.E. Zachara, G.W. Hart, Chem. Rev. 102 (2002) 431–438.
[6] R. Kikkeri, B. Lepenies, A. Adibekian, et al., J. Am. Chem. Soc. 131 (2009) 2110–2112.
[7] M. Gary-Bobo, Y. Mir, C. Rouxel, et al., Angew. Chem. Int. Ed. 123 (2011) 11627–11631.
[8] H. Sha, Y. Zhang, Y. Wang, et al., Biosens. Bioelectron. 124 (2019) 59–65.
[9] L. Jia, L.P. Lv, J.P. Xu, et al., J. Nanoparticle Res. 13 (2011) 4075–4083.
[10] Q. Sha, R. Guan, H. Su, et al., Talanta 218 (2020) 121130.
[11] L. Wang, K.Y. Pu, J. Li, et al., Adv. Mater. 23 (2011) 4386–4391.
[12] C.C. Huang, C.T. Chen, Y.C. Shiang, et al., Anal. Chem. 81 (2009) 875–882.
[13] C.F. Huang, G.H. Yao, R.P. Liang, et al., Biosens. Bioelectron. 50 (2013) 305–310.
[14] K. Yuan, H.M. Meng, Y. Wu, et al., CCS Chem. 4 (2022) 1597–1609.
[15] J.K. Ajish, A.B. Kanagare, K.S.A. Kumar, et al., ACS Appl. Nano Mater. 3 (2020) 1307–1317.
[16] H. Zhang, L. Zhang, R.P. Liang, et al., Anal. Chem. 85 (2013) 10969–10976.
[17] X. Zhang, F. Chen, X. Song, et al., Biosens. Bioelectron. 104 (2018) 27–31.
[18] S. Bhaskar, M. Moronshing, V. Srinivasan, et al., ACS Appl. Nano Mater. 3 (2020) 4329–4341.
[19] S. Bhaskar, A. Rai, K.M. Ganesh, et al., Langmuir 38 (2022) 12035–12049.
[20] A. Rai, S. Bhaskar, K.M. Ganesh, et al., Mater. Chem. Phys. 285 (2022) 126129.
[21] W.S. Tang, B. Zhang, L.D. Xu, et al., Analyst 147 (2022) 1873–1880.
[22] W. Song, Z.L. Song, Q. Li, et al., CCS Chem. 5 (2023) 176–190.
[23] X. Geng, Y. Sun, Z. Li, et al., Small 15 (2019) 1970259.
[24] Y. Shi, J. Liu, Y. Zhang, et al., Chin. Chem. Lett. 32 (2021) 3189–3194.
[25] J. Chen, N. Yuan, D. Jiang, et al., Chin. Chem. Lett. 32 (2021) 3398–3401.
[26] S. Bhaskar, N.S. Visweswar Kambhampati, K.M. Ganesh, et al., ACS Appl. Mater. Interfaces 13 (2021) 17046–17061.
[27] P. Shen, Y. Xia, Anal. Chem. 86 (2014) 5323–5329.
[28] Z. Qu, X. Zhou, L. Gu, et al., Chem. Commun. 49 (2013) 9830.
[29] Q. Chen, W. Wei, J.M. Lin, Biosens. Bioelectron. 26 (2011) 4497–4502.